M.J.Kadhim
Department of Production Engineering and Metallurgy, University of Technology, Baghdad, Iraq

M. H. Hafiz
Al-Iraqi University, Engineering College

M. A. Ali Bash
Department of Production Engineering and Metallurgy, University of Technology, Baghdad, Iraq.
soukaena.hassan@yahoo.com

Design and Evaluation of Zirconia Based Thermal Barrier Powders for Advanced Engines

Abstract- *Advanced utility, diesel and turbines engines used widely in aerospace, chemical and oil industries are based on plasma sprayed thermal barrier coatings. The successful performance of these coatings during servicing are relied mostly on the careful design, selection and analysis of zirconia-based ceramic powders stabilized with yttria and ceria. Different design of sampling techniques relevant for each evaluates property is a key factor to obtain reliable data. Significant property differences were observed for single and mixed powders. In the present work the particle size, its distribution, apparent density, flow rate, biased standard deviation, unbiased standard deviation and phases were characterized using sieving, flowmeter, scanning electron microscopy (SEM), X-ray diffraction (XRD), step scanning X-ray diffraction, energy dispersive spectroscopy (EDS), electron microprobe analysis (EPMA) and FT-IR. Two single alloyed zirconia powders of zirconia- 25 wt% CeO_2-2.5 wt% Y_2O_3 (Sulzer Metco 205NS) and zirconia- 8 wt% Y_2O_3 (Sulzer Metco 204NS-G) and mixture of these powders 80 wt% (Sulzer Metco 205NS) and 20 wt% (Sulzer Metco 204NS-G) were investigated. The particle shape has a remarkable effect on the flow rate and apparent density rather than the other properties. The particle distribution gives important noticeable information for the plasma spraying coatings.*

Keywords: *Advanced ceramic powder; Flow rate; Apparent density; Phases*

How to cite this article M.J.Kadhim., M. H. Hafiz.,and M. A. Ali Bash. "Design and Evaluation of zirconia based thermal barrier powders for advanced engines" *Engineering and Technology Journal*, Vol. 35, Part A, No. 10, pp. 1011-1024, 2017.

1.Introduction

Most zirconia based ceramic powder manufacturing techniques produced powders with broad primary characteristics [1]. These characteristics are shape, size, distribution, texture, chemical composition and purity [1,2]. These properties have significant effect on the secondary powder characteristics such as apparent density, specific surface and flow rate [3]. Therefore, careful design and selection procedures are required for sampling and evaluation to obtain reliable data for spraying coatings [4]. The sampling selection is the most important vital factor for spraying process especially for premixing ceramic powders to ensure the successful of evaluation [5].

They have been widely accepted the most reliable ceramic powders for plasma sprayed thermal barrier coatings are based on yttria partially stabilized zirconia (YPSZ) contain approximately 6.5 to 8.5 wt% yttria [6,7]. Recently, most interest works have been made on developing and characterization plasma sprayed coating contains 20 to 25 wt% ceria stabilized zirconia (CSZ) as candidates for YPSZ [8]. Analysis of these two systems (YPSZ and CSZ) showed that there are many interest suitable properties for each of them for thermal barrier coatings which may lead to develop many ternary systems [9,10].

It was well known that in spite of many physical and chemical interest properties of pure zirconia, no engineering bulk applications were used due to deleterious phase transformation. Therefore, advanced fields of stabilization zirconia were emerged during the last thirty five years or so. It is very important to mention that stabilizing of zirconia to control the tetragonal phase (t) to monoclinic phase (m) transformation were analyzed thoroughly in the first two important congresses of zirconia and its alloys [11,12] as well in many important reviews [13-15]. They have been accepted worldwide stabilizing of zirconia with yttria and ceria enjoy the benefit of control phase transformation to emerge many vital wide spread applications [17]. Stabilizing zirconia can be produced with many other oxides having very high melting points, chemical inertness,

https://doi.org/10.30684/etj.35.10A.8
2412-0758/University of Technology-Iraq, Baghdad, Iraq

oxidation resistance and high fracture toughness [17-19]. The type of stabilizing zirconia can be controlled by at least three important features; amount of oxide stabilizer, its type and cooling rate [20-22]. They were reported that more than fifteen oxides may add to stabilize zirconia for many advanced applications and the most one is thermal barrier coatings [23-25]. The most important are calcia, magnesia, yttria, ceria, Scandia, ytterbia, samaria, gadolina, lanathaa, holmia, erbia, dysposia, alumina, tantalia and hafania. Recently, great attentions and significant amount of work are carried out to the development of ternary systems based on zirconia-ceria-yttria as thermal barrier coating systems (CYSZ) [26]. These systems were produced from premixed of standard powders of zirconia-ceria and zirconia-yttria [27]. Due to the well agreed hypothesis that premixing is very important variable for successful thorough intermingling, careful design and evaluation of final premixed powders are needed.

The aim of this work was to determine the feasibility of sampling selection of primary and premixed zirconia based thermal barrier powders to describe the successful of final target of homogenous plasma sprayed coating. The paper reported that the new approach based on detail electron probe microanalysis (EPMA) is the most scientific tool to describe the degree of mixing efficiency for advanced powders.

2.Experimental Procedures

Three standard thermal barrier coatings powders namely Sulzer Metco 204NS-G (zirconia- 8 wt% yttria), Sulzer Metco 205NS (zirconia-25 wt% ceria- 2.5 wt% yttria) and mixture of these oxide powders with volume fractions of 80 wt% Sulzer Metco 205NS and 20 wt% Sulzer Metco 204NS-G were examined thoroughly to confirm the new approach. The nominal composition of mixed powder is approximately ZrO_2- 20 wt% CeO2- 3.6 wt% Y_2O_3. The standard fact sheet of Sulzer Metco 204NS and Sulzer Metco 205NS-G is listed in Table 1 [28,29]. The average supplier particle size for both Sulzer Metco 204NS-G and Sulzer Metco 205NS powders is +11 – 125 μm.

Great care was taken to select the represent sampling for the primary and mixed powder in order to improve accuracy for all investigated properties and the characteristics of the powders.

The particle size and its distribution of the three powders were determined by sieving process using standard sieves according to the ASTM B 214. The instrument has two dimensional movement, horizontally having circular motion and vertically for tapping. These movements are capable to be sufficient for particles to pass the given sieve size successfully. Six sieves with 200 mm diameter were used (10, 25, 53, 75, 106 and 112 μm respectively). In order to evaluate the powders accurately and controlling the statistical nature of the powders, careful sampling procedures were employed for the Sulzer Metco 204NS-G, 205NS and mixed powder. More attention was paid for mixed powder since it is the target for extra studies. To secure the successful of mixing, firstly careful samplings procedures based on ASTM B 215 were covered for the primary powders. . Samples of approximately 3.2 kg for Sulzer Metco 205NS and Sulzer Metco 204NS-G powders were taken from the lots of 5.7 kg for each powder to obtain the sampling (Fig. 1). Secondly, approximately, 400 g samplings were used for Sulzer Metco 204NS-G and Sulzer Metco 205NS while 500 g was used for premixed powder and the average of two samplings was evaluated. All samplings were selected based on cone and quartering sampling technique [30]. The chemical analyses of premixed powder were analyzed using EPMA from EDS equipped with scanning electron microscopy (SEM). The efficiency of mixing powder was determined from EPMA assessment of average area 600 x 600 μm for each mixing sample at a given interval time. Six samples of total weight 500 g powder were used for mixing samples using standard jar. Dry mixing was taken place for different interval times (15, 30, 60, 75, 90 and 120 min). The other variables of mixing were made constant. This is because the mixing time is the most important parameter covers the desired result. The small samples selected for EPMA analysis was done by thief technique. The biased variance (or unbiased variance) and biased standard deviation (or unbiased standard deviation) were determined from EPMA to describe the degree of efficiency of mixing. Six samples were selected and analyzed for each mixing time. The biased variance and biased standard deviations of mixed powder for CeO_2 and Y_2O_3 at different mixing times can be expressed mathematically by equations 1 and 2 respectively [31]:

$$\Sigma^2 = \sum_{i=1}^{n} \left(\frac{(X-Xi)2}{n} \right) \quad (1)$$

$$\Sigma^2 = \sum_{i=1}^{n} \left(\frac{(Y-Yi)2}{n} \right) \quad (2)$$

where S^2 is biased variance of mixed power; S is biased standard deviation of the mixed powder; n is number of EPMA analysis of samples; i is selected sample number; X or Y is the standard EPMA analysis of CeO_2 or Y_2O_3 respectively, X_i or Y_i is selected sample EPMA analysis of CeO_2 or Y_2O_3.It should be mentioned that the values of S^2

and S are similar for both CeO_2 and Y_2O_3. Therefore, the data reported are based on the CeO_2 analysis. For higher precision data to increase the reliability and certainty due to limited number of sample analysis (the average of six analysis was reported for each mixing time), the n value replaced by n – 1. In this case, the S^2 and S based on n-1 is termed unbiased variance and unbiased standard deviation respectively. The equations used then become [31]:

$$S^2=\sum_{i=1}^{n}\left(\frac{(X-Xi)2}{n-1}\right) \quad (3)$$

$$S^2=\sum_{i=1}^{n}\left(\frac{(Y-Yi)2}{n-1}\right) \quad (4)$$

Detailed analysis of the features obtained from standard evaluation of apparent density and flow rate for the three powders [30] showed the considerable variation. Hall flow meter based on ASTM B 212 and ASTM B 213 were applied to determine apparent density and flow rate respectively. Since, there were wide scatter of measured data; Weibulls distribution was employed to describe the reliable values rather than statistical average. More detail for the procedures of Weibull analysis can be found other else [32]. The phases of the primary powders and the mixed powder were determined from X-ray diffraction patterns recorded. SHIMADZU system diffractometer using CoKα and CuKα radiations at 40 kV and 40 mA were employed. The lattice parameters were calculated from the lowest range of angles (2θ 27.5 to 32.5°) for monoclinic phase (m) and from the highest range of angles (2θ 72 to 75.5°) for transformable tetragonal phase (t). The volume fractions of the phases present in the powders were measured from the area under the corresponding peaks according to Miller etal equations [33]. The error of volume fraction calculation is believed to be with ± 5 to 10%.

The FT-IR spectra have been recorded in the 4000-400 cm^{-1} with 0.5 cm^{-1} resolution. The FTIR spectra were recorded on highest SNs ratio IRAffinity-1S SHIMADZU Fourier Transform Infrared Spectrometer to determine the absorptivity of the mixed powders.

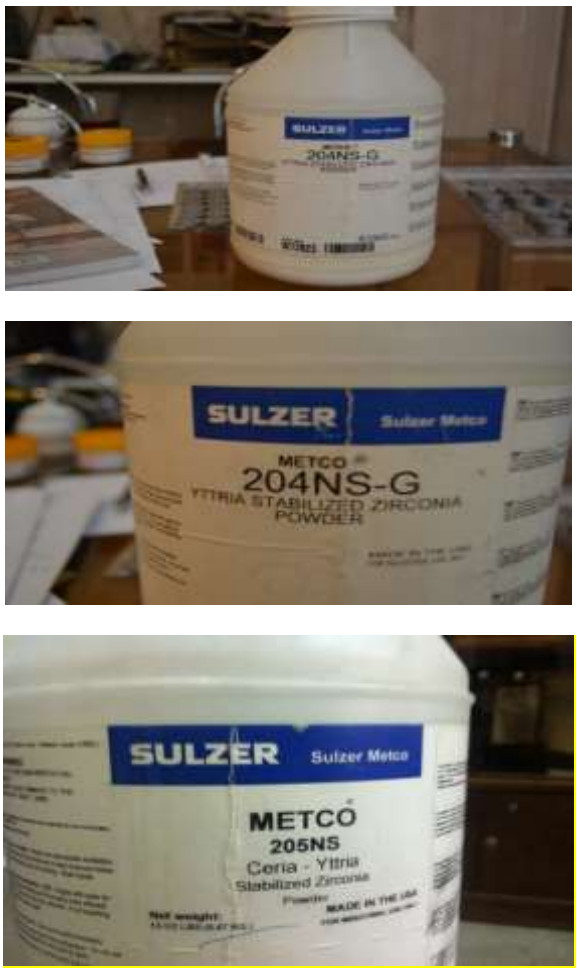

Figure 1: Standard Sulzer Metco 205NS and Sulzer Metco 204NS-G powders.

Table 1. Fact sheet of Sulzer Metco 204NS-G and Sulzer Metco 205NS powders.

Fact sheet	Sulzer Metco 204NS-G	Sulzer Metco 205NS
Classification	Ceramic, zirconia based	Ceramic, zirconia based
Chemistry	ZrO_2- 8 wt% Y_2O_3	ZrO_2-25 wt% CeO_2-2.5 wt% Y_2O_3
Manufacture	Agglomerated and HOSP™	Agglomerated and HOSP™
Morphology	Spheroidal	Spheroidal
Apparent density	2.3 ± 0.2 g/cm^3	2.2 ± 0.1 g/cm^3
Purpose	Thermal protection	Thermal barrier
Melting point	2800 °C (5072 °F)	
Service temperature	XCL products ≤ 1350 °C (2460 °F) Other products ≤ 1250 °C (2280 °F)	1250 °C (2280 °F)
Process	Atmospheric plasma spray, ChamPr™ (LVPS, LPPS, VPS)	Atmospheric plasma spray

Table 2 Particle size data for (a) Sulzer Metco 204NS-G, (b) Sulzer Metco 205NS and (c) the mixed powder.

(a)

Sieve size	wt 1, g	wt 2, g	Average wt, g	wt%	Cumulative less than%
10	28	26	27	6.7	6.7
25	34	39	36.5	9.1	15.8
53	150	143	146.5	36.4	52.2
75	73	86	79.5	19.8	72.0
106	86	81	83.5	20.8	92.8
112	25	33	29	7.2	100
Total	396	408	402	100	100

(b)

Sieve size	Wt1, g	Wt2, g	Average wt, g	wt%	Cumulative less than %
10	19	22	20.5	5.1	5.1
25	26	31	28.5	7.1	12.2
53	135	122	128.5	32	44.2
75	119	127	123	30.7	74.9
106	77	80	78.5	19.6	94.5
112	22	22	22	5.5	100
Total	398	404	401	100	100

(c)

Sieve size	Wt1, g	Wt2, g	Average wt, g	wt%	Cumulative less than %
10	32	30	31	6.3	5.1
25	40	44	42	8.5	12.2
53	172	178	175	35.4	44.2
75	122	119	120.5	24.3	74.9
106	103	97	100	20.2	94.5
112	28	24	26	5.3	100
Total	497	492	494.5	100	100

Table 3: The apparent density distribution of (a) Sulzer Metco 204NS-G, (b) Sulzer Metco 205NS and (c) mixed powder. (a)

Reading Number	Apparent density, g/cm^3	ln apparent density	S_i	$1/S_i$	$\ln 1/S_i$	$\ln\ln 1/S_i$	m	App. density at 37% S_i, g/cm^3
1	2.37	0.8628	0.066	15.151	2.718	0.999	25.42	2.285
2	2.37	0.8628	0.133	7.518	2.017	0.701		
3	2.32	0.8415	0.2	5	1.609	0.475		
4	2.3	0.8329	0.266	3.759	1.324	0.280		
5	2.29	0.8285	0.333	3.003	1.099	0.094		
6	2.28	0.8241	0.4	2.5	0.916	-0.087		
7	2.26	0.8153	0.466	2.145	0.763	-0.269		
8	2.25	0.8109	0.533	1.876	0.629	-0.463		
9	2.21	0.7929	0.6	1.666	0.510	-0.671		
10	2.19	0.7839	0.666	1.501	0.406	-0.900		
11	2.16	0.7701	0.733	1.364	0.310	-1.169		
12	2.15	0.7654	0.8	1.25	0.223	-1.499		
13	2.13	0.7561	0.866	1.154	0.143	-1.938		

14	2.07	0.7275	0.933	1.071	0.069	-2.668		

(b)

Reading number	Apparent density, g/cm^3	ln apparent density	S_i	$1/S_i$	$\ln 1/S_i$	$\ln\ln 1/S_i$	m	App. density at 37%, g/cm^3
1	2.22	0.7975	0.066	15.151	2.718	0.999	22.36	2.078
2	2.14	0.7608	0.133	7.518	2.017	0.701		
3	2.12	0.7514	0.2	5	1.609	0.475		
4	2.1	0.7419	0.266	3.759	1.324	0.280		
5	2.09	0.7371	0.333	3.003	1.099	0.094		
6	2.06	0.7227	0.4	2.5	0.916	-0.087		
7	2.05	0.7178	0.466	2.145	0.763	-0.269		
8	2.04	0.7129	0.533	1.876	0.629	-0.463		
9	2.01	0.6981	0.6	1.666	0.510	-0.671		
10	1.99	0.6881	0.666	1.501	0.406	-0.900		
11	1.98	0.6830	0.733	1.364	0.310	-1.169		
12	1.93	0.6575	0.8	1.25	0.223	-1.499		
13	1.92	0.6523	0.866	1.154	0.143	-1.938		
14	1.88	0.6312	0.933	1.071	0.069	-2.668		

(c)

Reading number	Apparent density, g/cm^3	ln apparent density	S_i	$1/S_i$	$\ln 1/S_i$	$\ln\ln 1/S_i$	m	App. density at 37%, g/cm^3
1	2.24	0.8064	0.066	15.151	2.718	0.999	21.43	2.184
2	2.23	0.8020	0.133	7.518	2.017	0.701		
3	2.22	0.7975	0.2	5	1.609	0.475		
4	2.2	0.7884	0.266	3.759	1.324	0.280		
5	2.19	0.7839	0.333	3.003	1.099	0.094		
6	2.18	0.7793	0.4	2.5	0.916	-0.087		
7	2.17	0.7747	0.466	2.145	0.763	-0.269		
8	2.15	0.7654	0.533	1.876	0.629	-0.463		
9	2.12	0.7514	0.6	1.666	0.510	-0.671		
10	2.08	0.7323	0.666	1.501	0.406	-0.900		
11	2.02	0.7030	0.733	1.364	0.310	-1.169		
12	1.99	0.6881	0.8	1.25	0.223	-1.499		
13	1.98	0.6830	0.866	1.154	0.143	-1.938		
14	1.96	0.6729	0.933	1.071	0.069	-2.668		

Table 4: The flow rate distribution of (a) Sulzer Metco 204NS-G, (b) Sulzer Metco 205NS and (c) mixed powder.

(a)

Reading number	Flow rate, s/50 g	ln flow rate	S_i	$1/S_i$	$\ln 1/S_i$	$\ln\ln 1/S_i$	m	Flow rate at 37% S_i, s/50 g
1	68	4.2195	0.066	15.151	2.718	0.999		
2	66	4.1896	0.133	7.518	2.017	0.701		
3	63	4.1431	0.2	5	1.609	0.475		
4	58	4.0604	0.266	3.759	1.324	0.280	4.282	54
5	55	4.0073	0.333	3.003	1.099	0.094		
6	53	3.9702	0.4	2.5	0.916	-0.087		
7	49	3.8918	0.466	2.145	0.763	-0.269		
8	46	3.8286	0.533	1.876	0.629	-0.463		
9	45	3.8066	0.6	1.666	0.510	-0.671		
10	41	3.7135	0.666	1.501	0.406	-0.900		
11	39	3.6635	0.733	1.364	0.310	-1.169		
12	37	3.6109	0.8	1.25	0.223	-1.499		
13	35	3.5553	0.866	1.154	0.143	-1.938		
14	33	3.4965	0.933	1.071	0.069	-2.668		

(b)

Reading number	Flow rate, s/50 g	ln flow rate	S_i	$1/S_i$	$\ln 1/S_i$	$\ln\ln 1/S_i$	m	Flow rate at 37%, s/50 g
1	71	٤.٢٦٢٦	0.066	15.151	2.718	0.999		
2	70	٤.٢٤٨٥	0.133	7.518	2.017	0.701		
3	66	٤.١٨٩٦	0.2	5	1.609	0.475		
4	63	٤.١٤٣١	0.266	3.759	1.324	0.280		
5	60	٤.٠٩٤٣	0.333	3.003	1.099	0.094	3.788	58
6	56	٤.٠٢٥٣	0.4	2.5	0.916	-0.087		
7	55	٤.٠٠٧٣	0.466	2.145	0.763	-0.269		
8	53	٣.٩٧٠٢	0.533	1.876	0.629	-0.463		
9	51	٣.٩٣١٨	0.6	1.666	0.510	-0.671		
10	47	٣.٨٥٠١	0.666	1.501	0.406	-0.900		
11	45	٣.٨٠٦٦	0.733	1.364	0.310	-1.169		
12	38	٣.٦٣٧٥	0.8	1.25	0.223	-1.499		
13	32	٣.٤٦٥٧	0.866	1.154	0.143	-1.938		
14	30	٣.٤٠١٢	0.933	1.071	0.069	-2.668		

(c)

Reading umber	Flow rate, s/ 50 g	ln flow rate	S_i	$1/S_i$	$\ln 1/S_i$	$\ln\ln 1/S_i$	m	Flow rate at 37%, s/50 g
1	73	٤.٢٩٠٤	0.066	15.151	2.718	0.999		
2	66	٤.١٨٩٦	0.133	7.518	2.017	0.701		
3	64	٤.١٥٨٨	0.2	5	1.609	0.475		
4	61	٤.١١٠٨	0.266	3.759	1.324	0.280		
5	57	٤.٠٤٣٠	0.333	3.003	1.099	0.094		
6	52	٣.٩٥١٢	0.4	2.5	0.916	-0.087		
7	47	٣.٨٥٠١	0.466	2.145	0.763	-0.269		
8	46	٣.٨٢٨٦	0.533	1.876	0.629	-0.463		
9	43	٣.٧٦١٢	0.6	1.666	0.510	-0.671	3.76	55
10	39	٣.٦٦٣٥	0.666	1.501	0.406	-0.900		
11	38	٣.٦٣٧٥	0.733	1.364	0.310	-1.169		
12	36	٣.٥٨٣٥	0.8	1.25	0.223	-1.499		
13	34	٣.٥٢٦٣	0.866	1.154	0.143	-1.938		
14	31	٣.٤٣٣٩	0.933	1.071	0.069	-2.668		

Table 5: Typical %mole of m, t, c and t' for 204NS-G, 205NS and mixed powders.

Ceramic type	mole% m	mole% c	mole% t	mole% t'
Metco 204NS-G powder	16 ± 2	nil	84 ± 2	nil
Metco 205NS powder	16 ± 2	nil	84 ± 2	nil
Mixed powder	16 ± 2	nil	84 ± 2	nil

Table 6: Lattice parameters of t phase and relative intensity of m and t phases.

Parameter	Value
a, nm	0.5132
c, nm	0.5234
c/a ratio	1.0198
$I_t(004)/(400)$	0.4-0.6
$\Delta 2\theta${400 range} t	1.2-1.3
$\Delta 2\theta${400 range} t'	-
$I_m(ì11)/ I_m(111)$	1.6

Table 7:Values of biased variance, unbiased variance, biased standard deviation and unbiased standard deviation of mixed powder at different mixing time.

Mixing time, min	Biased S^2	Biased S	Unbiased S^2	Unbiased S
0				
15	4.3	2.07	5.2	2.28
30	3.2	1.79	3.8	1.95
60	2.0	1.41	2.4	1.55
75	2.8	1.67	3.4	1.84
90	3.2	1.79	3.8	1.95
120	3.3	1.82	4	2

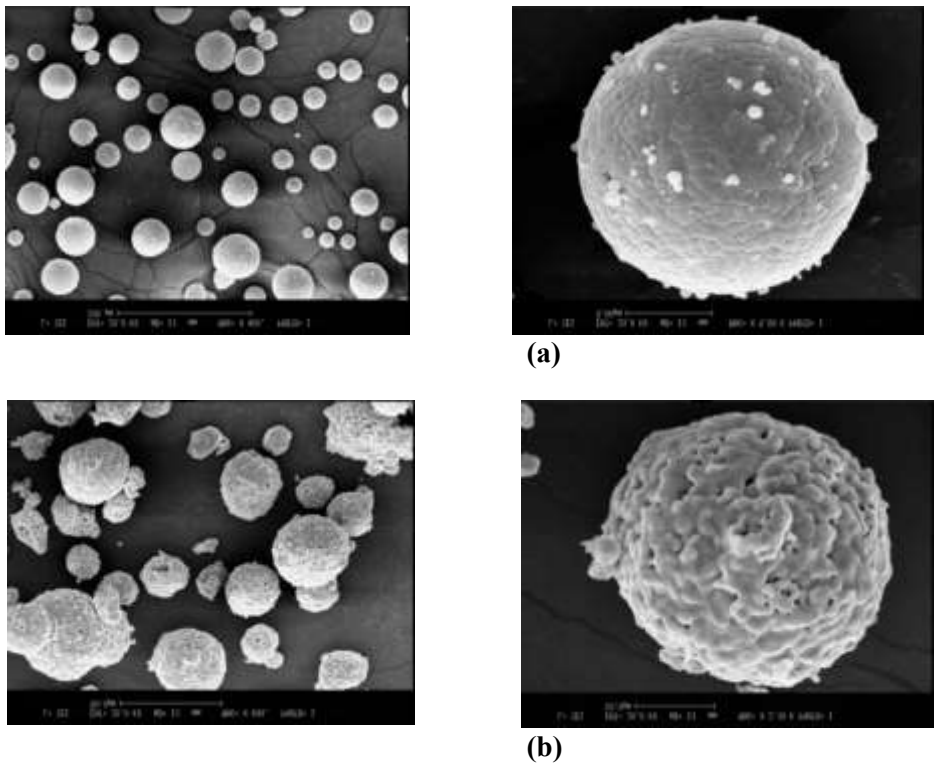

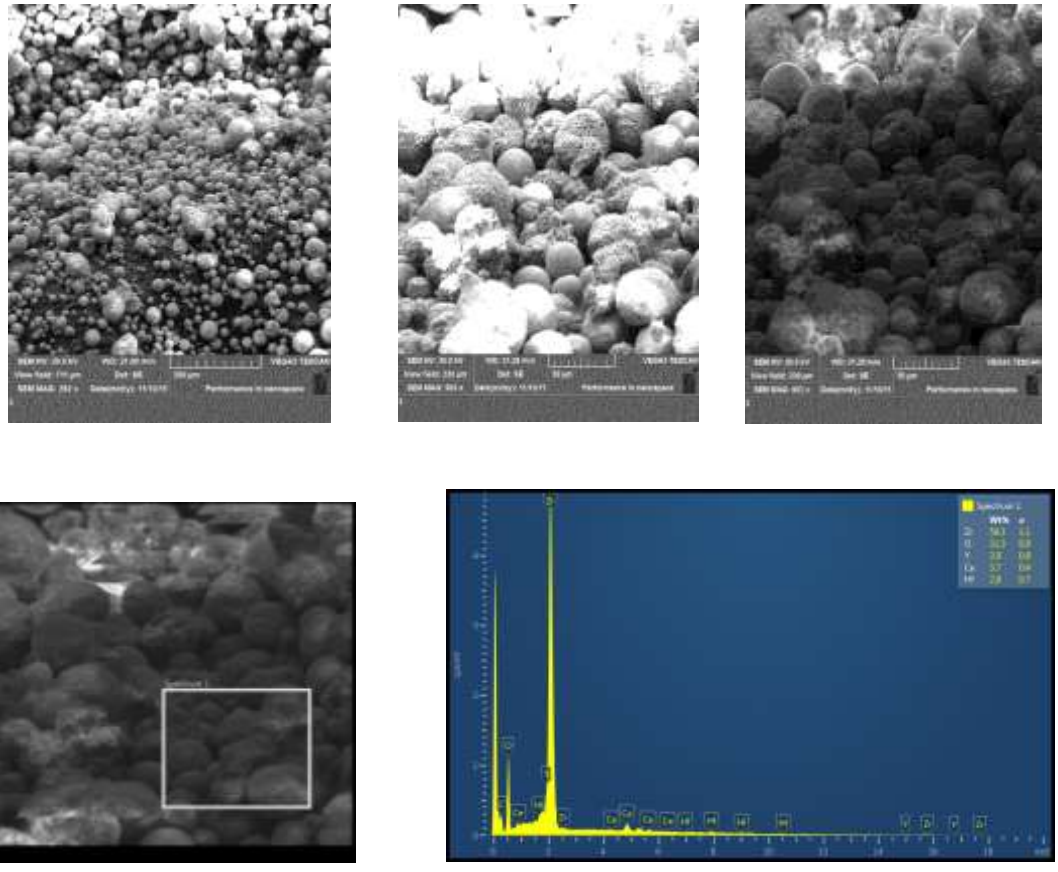

Figure 2: SEM micrographs of typical (a) Sulzer Metco 205NS, (b) Sulzer Metco 204NS-G and (c) mixed Sulzer Metco 205NS and Sulzer Metco 204NS-G powder and (d) EDS of mixed powder.

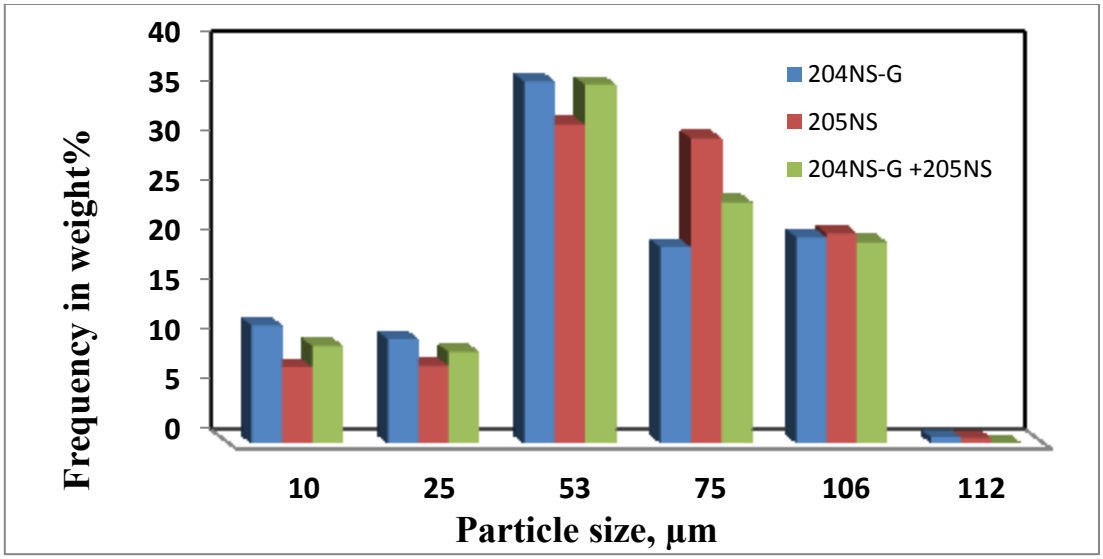

(a)

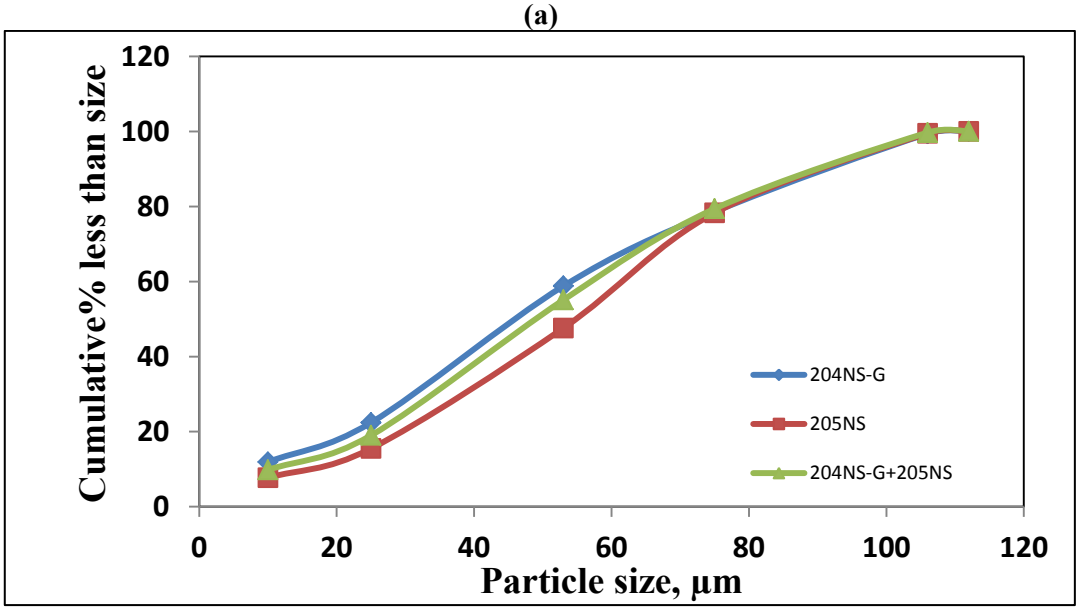

(b)

Figure 3: Histogram and size distribution for the powders investigated (a) and (b) cumulative% less than size.

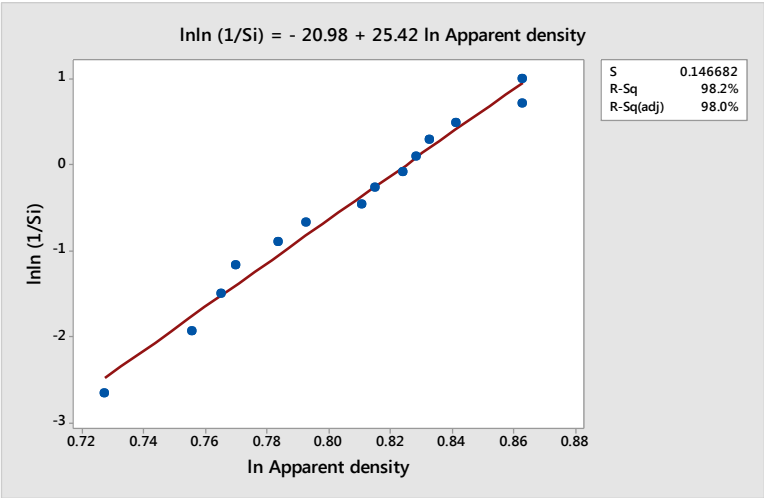

(a)

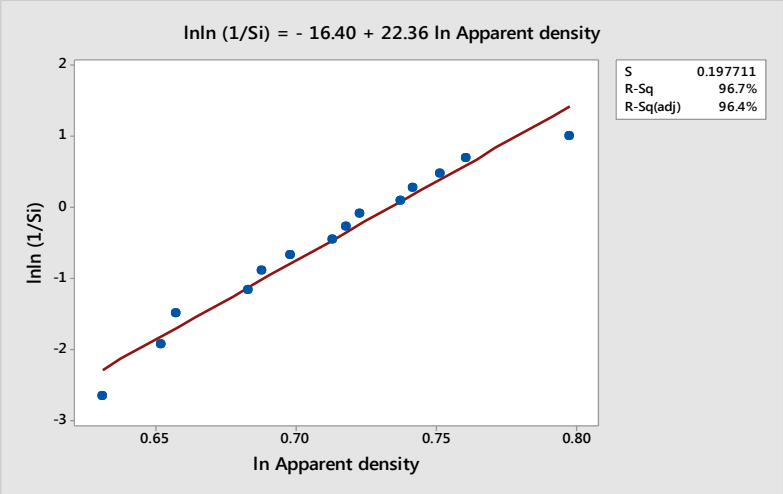

(b)

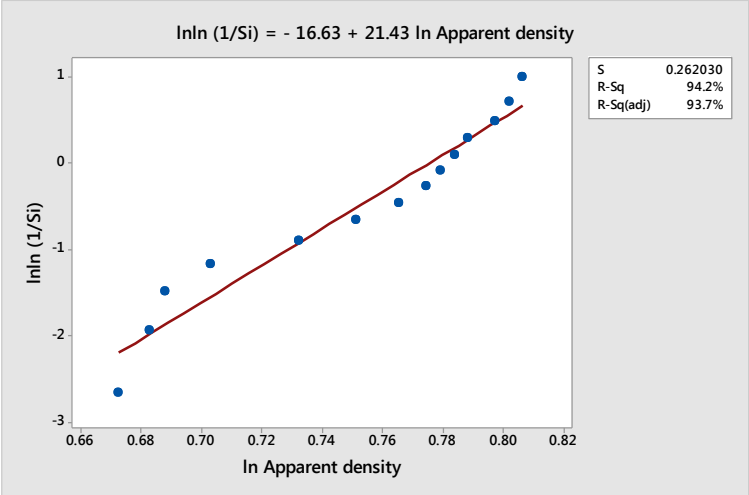

(c)

Figure 4: Weibull's modulus for (a) 204NS-G, (b) 205NS and (c) mixed 204NS-G and 205NS powders.

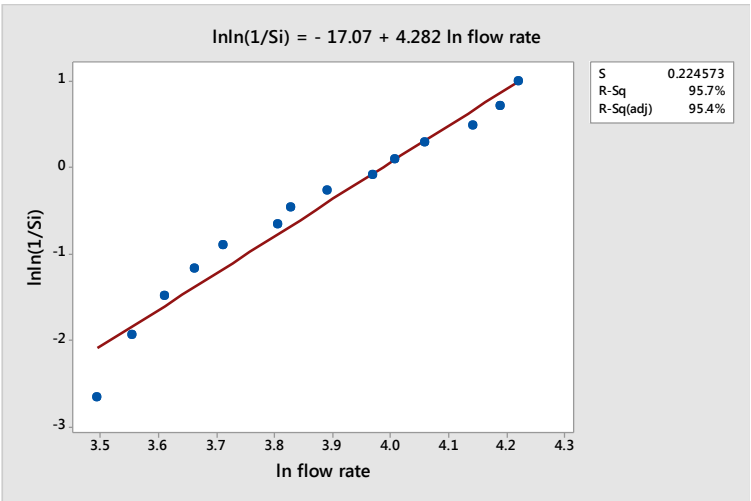

(a)

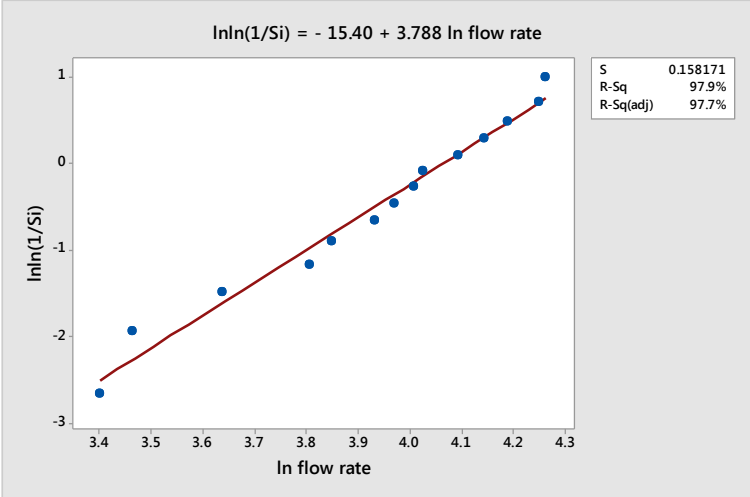

(b)

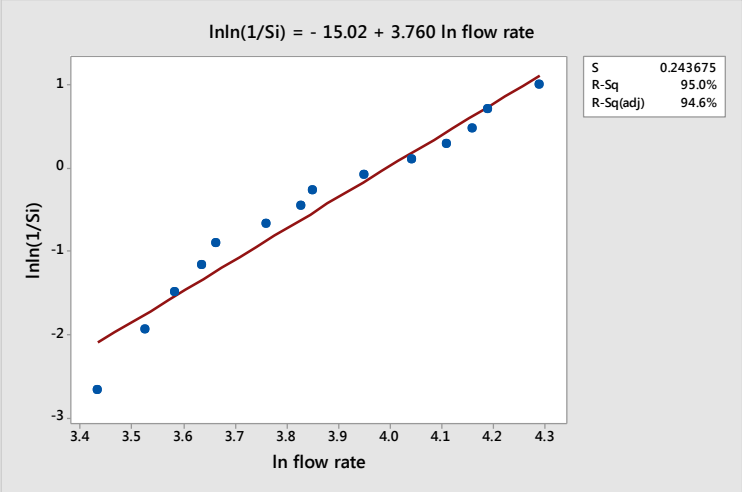

(c)

Figure 5: Weibull's modulus for (a) 204NS-G, (b) 205NS and (c) mixed 204NS-G and 205NS powders.

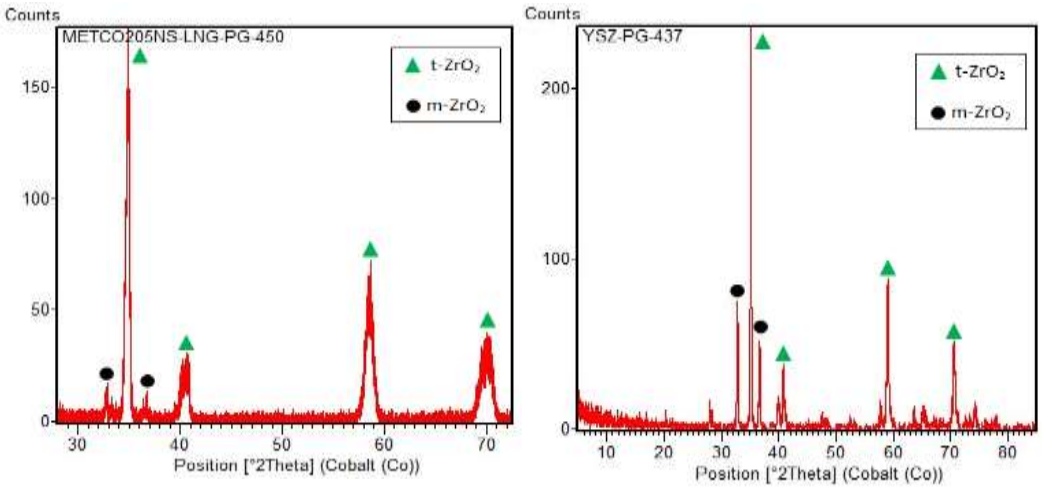

(a) **(b)**

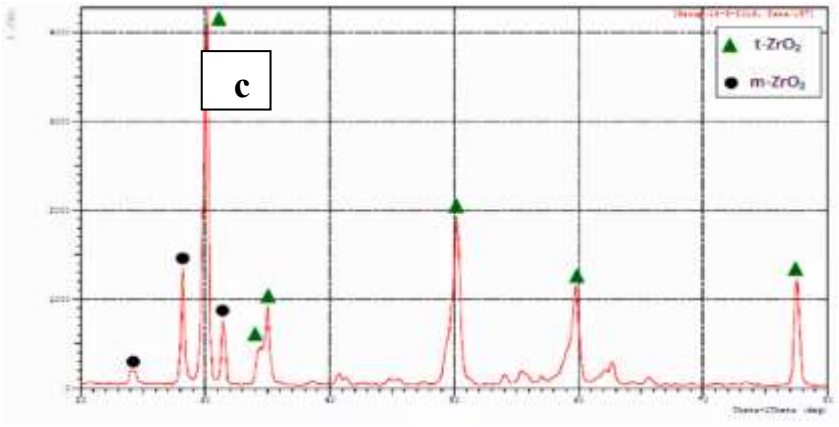

(c)

Figure 6: XRD pattern of (a) Sulzer Metco 205NS powder, (b) Sulzer Metco 204NS-G and (c) Mixed powder of Sulzer Metco 205Ns and Sulzer Metco 204NS-G. Note (a) and (b) Co radiation while (c) Cu radiation.

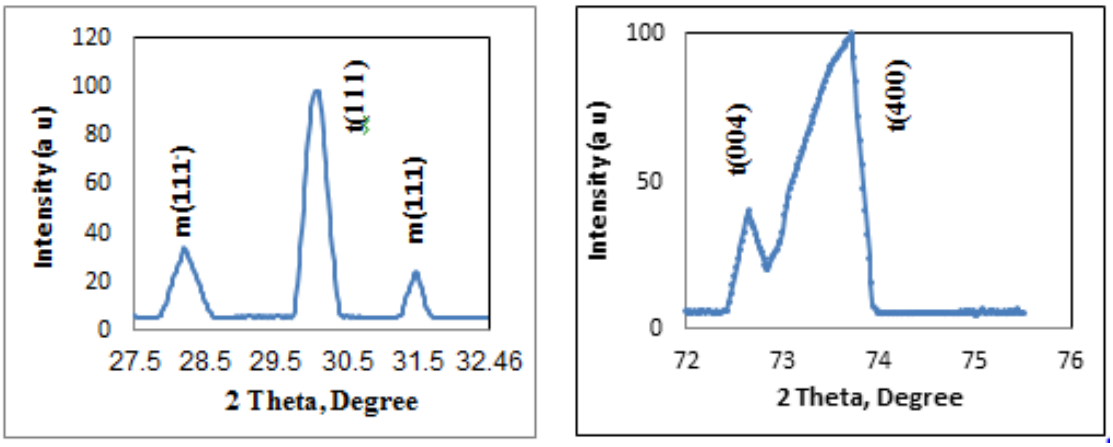

Figure7: Step scanning for mixed Sulzer Metco 204NS-G and Sulzer Metco 205NS powder.

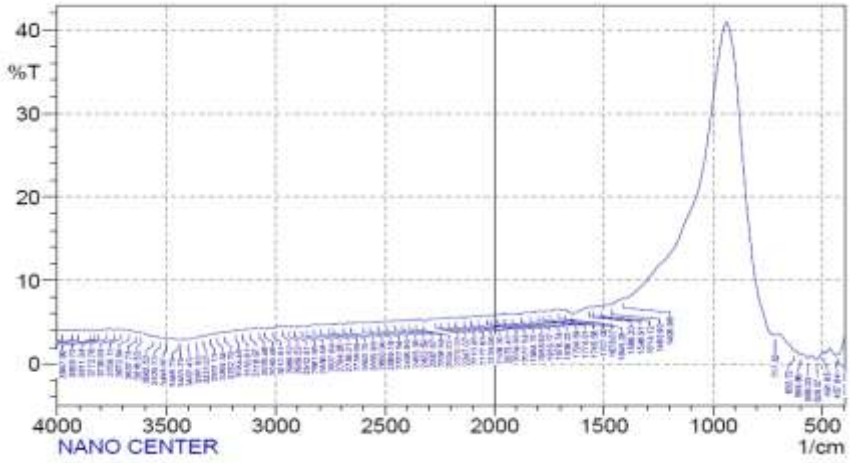

(a)

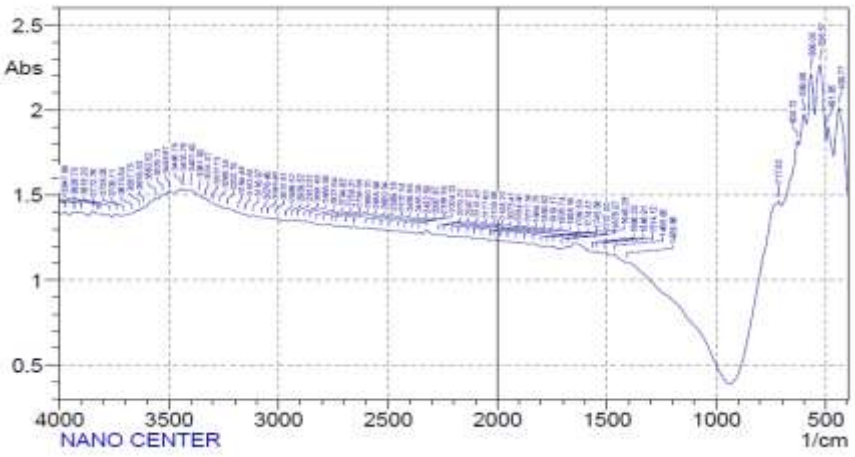

(b)

Figure 8: FT-IR spectrum of mixed Sulzer Metco 204NS-G and Sulzer Metco 205NS powder in the range of 4000-430 cm^{-1} (a) % transmission and (b) absorption.

Conclusions

1- Scientific careful designing of sampling selection of advanced powders is the important key factor to obtain the reliable data to be considered further for advanced processing.

2- Weibull's distribution modulus can be used effectively to describe the primary and secondary powder characteristics.

3- EPMA is the most powerful analytical chemical tool to describe the degree of efficiency of mixing powder.

4- The degree of mixing is very lengthy and requires accurate chemical analysis.

5- A new approach is examined to be important to be implemented in analysis of advanced ceramic mixing powders.

References

[1]G.Y. Guo, Y.L. Chen, High-quality zirconia powder resulting from the attempted separation of acetic acid from acrylic acid with zirconium oxychloride, J. of Materials Chemistry, 11(2001)1283-1287.

[2]J. Calado, Ceramic powder production with emulsion detonation synthesis, Cfi/Ber. DKG 93(2016)4-5.

[3]G.Dowson, Powder Metallurgy the Process and its Products, Adam Hilger, Bristol and New York, 1990.

[4]M. Oksa , E. Turunen, T. Suhonen, T. Varis, S.P. Hannula, Optimization and characterization of high velocity oxy-fuel sprayed coatings, Techniques, Materials and Applications Coatings, 1(2011)17-52.

[5]M.K. A1 Mamun, Design and development of a powder mixing device used in the deposition of high velocity oxy-fuel (HVOF) thermal spray functionally graded coatings, MSc thesis, 2007.

[6]S. Ilina, G. Ionescu, V. Manoliu, R. R. Piticescu, Nanostructured zirconia layers as thermal barrier coatings, Incas Bulletin, 3(2011)63- 69.

[7]B. Lu, D. Wang, L. Xiao, F. Li, J. Ren, L. Li, W. Wu, Microstructure analysis of laser remelting for thermal barrier coatings on the surface of titanium alloy, MATEC Web of Conferences 67, 04019 (2016).

[8]A. Anderson, An investigation of the thermal shock behavior of thermal barrier coatings, International Journal of Engineering Science and Technology, 3(2011)8154-8158.

[9]E.Y. Lee,Y.Sohn, S.K. Jha, J.W. Holmes, R.D. Sisson Jr, Phase transformation of plasma-sprayed zirconia-ceria thermal barrier coatings, J. of the American Ceramic Society, 85(2002)2065-2071.

[10] M.R. Rahimipour, M.S. Mahdipoor, Comparative study of plasma sprayed yattria and ceria stabilized zirconia properties, IJE Transactions A: Basics 26(2013)13-18.

[11] X.Q. Cao, R. Vassen, D. Stoever, Ceramic materials for thermal barrier coatings, Journal of the European Ceramic Society 24(2004)1-10.

[12] Advances in ceramics, Vol. 3, (Science and technology of zirconia, Eds., A.H. Heuer, L.W. Hoobs, Published by the American Ceramic Society, (ACerS), USA, 1981.

[13] Advances in ceramics, Vol. 24, Science and Technology of zirconia, Eds., S.Somiya, N. Yamamoto, H. Yanagida, Published by the American Ceramic Society, (ACerS), USA, 1988.

[14] H. Canan U. and L. Yuk-Chiu, Advances in thermal spray coatings for gas turbines and energy generation: A review, Journal of Thermal Spray Technology, 22(2013)564-576.

[15] A.S. Asharaf, K. Sume, D. Mangala, M. Ranjana, Zirconia: properties and application: A review, Pakistan Oral and Dental Journal, 34(2014)178.

[16] R.H.J. Hannink, P.M Kelly, B.C. Muddle, Transformation toughening in zirconia-containing

ceramics, J. of the American Ceramic Society, 83(2000)461-487.
[17] S.H. Guo, H. Peng, S. Gong, H. Xu, Phase stability and thermal conductivity of ytterbia and yttria co-doped zirconia, Progress in Natural Science: Materials International, 23(2013)440-445.
[18] G. Sattonnay , S. Moll, V. Desbrosses, V.M. Bekale, C. Legros, L. Thomé, I. Monnet, Mechanical properties of fluorite-related oxides subjected to swift ion irradiation: Pyrochlore and zirconia, Nuclear Instruments and Methods in Physics Research B, 268(2010)3040-3043.
[19] P. Thangadurai, V. Sabarinathan, A.C. Bose1, S. Ramasamy, Conductivity behaviour of a cubic/tetragonal phase stabilized nanocrystalline La_2O_3–ZrO_2, Journal of Physics and Chemistry of Solids, 65(2004)1905-1912.
[20] F.I. Zhou, Y. Wang, L. Wang, Z. Cui, Z. Zhang, High temperature oxidation and insulation behavior of plasma-sprayed nanostructured thermal barrier coatings, Journal of Alloys and Compounds, 704(2017)614-623.
[21] K.A. Khor, J. Yang, Transformability of t-ZrO_2 and lattice parameters in plasma sprayed rare earth oxides stabilized zirconia coatings, Scripta Materialia, 37(1997)1279-1286.
[22] M. Balkenhol, F.P. Nothdurft, M. Hannig, A.l Schindler, A. Lehmann, T. Arnold, A. Knauber, S. Rupf, Bonding to zirconia ceramic: The effect of cold plasma treatment and 4-META, Clinical Plasma Medicine, 5-6(2017)8-13.
[23] A.P. Bechepeche, O. Treu Jr, E. Longo, C.O. Paiva-Santos, J.A. Varela, Experimental and theoretical aspects of the stabilization of zirconia, J. of Materials, 34(1999)2751-2756.
[24] J.H. Glenn, Scandia-and-yttria-stabilized zirconia for thermal barriers, NASA Tech Briefs, Research Center, Cleveland, Ohio, October 2003.
[25] J. Fenech, M. Dalbin, A. Barnabe, J.P. Bonino, F. Ansart, Sol–gel processing and characterization of (RE-Y)- zirconia powders for thermal barrier coatings, Powder Technology, 208(2011)480-487
[26] M. Karabaş, E. Bal, A. Kilic, İ.Y. Taptık, Effect of air plasma spray parameters on the Properties of YSZ and CYSZ thermal barrier coatings, Journal of the Australian Ceramic Society, 52(2016)175-182.
[27] N. Khan, B.C.H. Steele, ZrO_2-CeO_2-Y_2O_3: electrical and mechanical property relationships with the microstructure, Materials Science and Engineering B, 8(1991)265- 271.
[28] Material product data sheet 8 % yttria stabilized zirconia agglomerated and HOSP thermal spray powders, 2014, Oerlikon Metco. https://www.oerlikon.com
[29] Material product data sheet ceria-yttria stabilized zirconium oxide HOSP Powder, 2014, Oerlikon Metco. https://www.oerlikon.com
[30] ASM Metals Handbook, Vol. 7, Powder Metallurgy, 9th Ediation, 1984.
[31] J.J. Fisher, Solid-solid blending, Chemical Engineering, 1960, pp 107-128.
[32] Maryam Abduladheem Ali Bash, Optimizing, Phase transformation and hot corrosion resistance of laser sealing plasma sprayed ceria stabilized zirconia thermal barrier coatings, Ph.D. Thesis, Department of Production Engineering and Metallurgy, University of Technology, Baghdad, Iraq, 2017.
[33] R.A. Miller, J.L. Smaliek. G.G. Garlick, Phase stability in plasma sprayed partially stabilized zirconia-yttria, in Advances in Ceramics, Vol. 3. Edited by A.H. Heuer and L.W. Hobbs, The American Ceramic Society, Columbus, OH, 1981, pp 241-253.
[34] J.I. Eldridgew, C.M. Spuckler, Determination of scattering and Aabsorption coefficients for plasma-sprayed yttria-stabilized zirconia thermal barrier coatings, J. of the American Ceramic Society, 91(2008)1603-1611.
[35] S. Damyanova , B. Pawelec, K. Arishtirova, M.V. . Huerta, J.L.G. Fierro, Study of the surface and redox properties of ceria–zirconia oxides, Applied Catalysis A: General, 337(2008)86-96.